

# High-Fat Diet Modulates Hepatic Amyloid $\beta$ and Cerebrosterol Metabolism in the Triple Transgenic Mouse Model of Alzheimer's Disease

Cristina R. Bosoi <sup>1,3</sup>, Milène Vandal,<sup>3,4</sup> Marine Tournissac,<sup>3-5</sup> Manon Leclerc,<sup>3,4</sup> Hortense Fanet,<sup>3-5</sup> Patricia L. Mitchell,<sup>1</sup> Mélanie Verreault,<sup>6</sup> Jocelyn Trottier,<sup>6</sup> Jessica Virgili,<sup>3,4</sup> Cynthia Tremblay,<sup>3</sup> H. Robert Lippman,<sup>7,8</sup> Jasmohan S. Bajaj <sup>7,8</sup>, Olivier Barbier,<sup>4,6</sup> André Marette,<sup>1,2</sup> and Frédéric Calon <sup>3-5</sup>

Obesity and diabetes are strongly associated not only with fatty liver but also cognitive dysfunction. Moreover, their presence, particularly in midlife, is recognized as a risk factor for Alzheimer's disease (AD). AD, the most common cause of dementia, is increasingly considered as a metabolic disease, although underlying pathogenic mechanisms remain unclear. The liver plays a major role in maintaining glucose and lipid homeostasis, as well as in clearing the AD neuropathogenic factor amyloid- $\beta$  ( $A\beta$ ) and in metabolizing cerebrosterol, a cerebral-derived oxysterol proposed as an AD biomarker. We hypothesized that liver impairment induced by obesity contributes to AD pathogenesis. We show that the AD triple transgenic mouse model (3xTg-AD) fed a chow diet presents a hepatic phenotype similar to nontransgenic controls (NTg) at 15 months of age. A high-fat diet (HFD), started at the age of 6 months and continued for 9 months, until sacrifice, induced hepatic steatosis in NTg, but not in 3xTg-AD mice, whereas HFD did not induce changes in hepatic fatty acid oxidation, *de novo* lipogenesis, and gluconeogenesis. HFD-induced obesity was associated with a reduction of insulin-degrading enzyme, one of the main hepatic enzymes responsible for  $A\beta$  clearance. The hepatic rate of cerebrosterol glucuronidation was lower in obese 3xTg-AD than in nonobese controls ( $P < 0.05$ ) and higher compared with obese NTg ( $P < 0.05$ ), although circulating levels remained unchanged. **Conclusion:** Modulation of hepatic lipids,  $A\beta$ , and cerebrosterol metabolism in obese 3xTg-AD mice differs from control mice. This study sheds light on the liver-brain axis, showing that the chronic presence of NAFLD and changes in liver function affect peripheral AD features and should be considered during development of biomarkers or AD therapeutic targets. (*Hepatology Communications* 2021;5:446-460).

**N**onalcoholic fatty liver disease (NAFLD) is the most common cause of chronic liver disease.<sup>(1)</sup> NAFLD is associated with various features of metabolic syndrome such as obesity, type 2 diabetes, and cardiovascular diseases. All of these conditions present with cognitive impairment, and their

presence in midlife is recognized a risk factor for later development of Alzheimer's disease (AD), the most common cause of dementia.<sup>(2,3)</sup>

NAFLD is independently associated with lower cognitive performance,<sup>(4)</sup> affecting different types of memory. Patients with NAFLD exhibit difficulty

*Abbreviations:* 24S-OH-C, 24S-hydroxycholesterol; 24S-OH-C-24G, 24S-hydroxycholesterol-24glucuronide; 24S-OH-C-3S,24G, 24S-hydroxycholesterol-3sulfate-24glucuronide; 3xTg-AD, triple transgenic Alzheimer's disease mouse model; Abca1, ATP-binding cassette transporter (member 1 of human transporter subfamily); ACC, acetyl-CoA carboxylase; ACE2, angiotensin-converting enzyme2; AD, Alzheimer's disease; ALT, alanine aminotransferase; ANOVA, analysis of variance; APP,  $A\beta$  precursor protein; AST, aspartate aminotransferase;  $A\beta$ , amyloid beta; CD, control diet; cDNA, complementary DNA; Cpt1a, carnitine palmitoyltransferase 1a; eEF2, eukaryotic elongation factor 2; eWAT, epididymal adipose tissue; FAS, fatty acid synthase; G6pc, glucose-6-phosphatase; HFD, high-fat diet; Hmgcr, 3-hydroxy-3-methylglutaryl-CoA reductase; IDE, insulin-degrading enzyme; LC/MS-MS, liquid chromatography-tandem mass spectrometry; LRP1, low-density lipoprotein receptor-related protein 1; mRNA, messenger RNA; NAFLD, nonalcoholic fatty liver disease; NEP, neprilysin; ns, not significant; NTg, nontransgenic; Pck1, phosphoenolpyruvate carboxykinase 1; Ppara, peroxisome proliferator-activated receptor alpha; Ppargc1a, peroxisome proliferative activated receptor, gamma, coactivator 1 alpha; PS1, presenilin-1; Srebf1/2, sterol regulatory element-binding transcription factor 1/2; TG, triglyceride; UGT1A, UDP glucuronosyltransferase family 1 member A.

Received April 3, 2020; accepted August 20, 2020.

with delayed memory recall, assessed by the Montreal Cognitive Assessment Test<sup>(5)</sup> and lower performance in the Serial Digit Learning Test,<sup>(6)</sup> as compared with healthy controls. Failing performances in the same or similar tests probing for memory loss is an essential characteristic of AD. In addition, altered hepatic markers have been observed in AD mouse models<sup>(7)</sup> and patients with AD.<sup>(8,9)</sup> Dysregulation of the liver–brain axis of neurodegeneration as a result of impaired liver lipid metabolism has already been described in AD,<sup>(10)</sup> but studies investigating the association between AD and liver-related metabolic status are still lacking.

Peripheral metabolic alterations including defective insulin signaling are often present in animal models of AD<sup>(11,12)</sup> and patients with AD.<sup>(10,13)</sup> Because insulin regulates major pathways in the liver, such as gluconeogenesis, lipolysis and lipogenesis, a significant metabolic impact is to be expected. Indeed, Tang et al. reported a hepatic substrate shift from lipogenesis toward glucose production following a high-fat diet (HFD) in an animal model of AD neuropathology, thus contributing to glucose intolerance.<sup>(12)</sup>

Amyloid  $\beta$  ( $A\beta$ ) is the main component of the amyloid plaques found in the brain of patients with AD. The peptide is excreted from the brain into the circulation, with the liver being an important  $A\beta$  clearing organ.<sup>(14)</sup> Although the liver plays a key role in the clearance of  $A\beta$  once in the periphery, its impact on the AD-related amyloidogenic cascade is still largely unexplored.

Increased levels of cerebrosterol (24S-hydroxycholesterol, 24S-OH-C) have been described in the brain, the cerebrospinal fluid, and in the circulation of patients with AD, although studies show conflicting results.<sup>(15,16)</sup> Cerebrosterol represents the principal form of cholesterol elimination from the brain and is metabolized by the liver: About 50% is glucuronidated to conjugated derivatives such as 24S-OH-C-24glucuronide (24S-OH-C-24G) and 24S-OH-C-3sulfate-24glucuronide (24S-OH-C-3S, 24G), while the remaining 50% is converted into bile acids.<sup>(17)</sup> 24S-OH-C-24G and 24S-OH-C-3S,24G are the most abundant circulating metabolites of cerebrosterol. These two metabolites are formed in the liver by cerebrosterol glucuronidation and sulfation,

*This study was made possible by funding from the Canadian Institutes of Health Research to FC (CIHR, MOP 102532 and LAO 74443) and AM (FDN-143247), the Natural Sciences and Engineering Research Council of Canada (NSERC, RGPIN 435555-2013, RGPGP 402213 2012), the Alzheimer Society Canada, the Fondation du CHU de Québec (Barbier's family gift), the Canada Foundation for Innovation (CFI) and VA Merit review I0CX001076. FC was supported by research scholar awards from the FRQS. AM was supported by a Pfizer/CIHR research Chair on the pathogenesis of insulin resistance and cardiovascular diseases. CRB was supported by a FRQS and an IUCPQ postdoctoral scholarship. MV was supported by a CIHR and an AIHS postdoctoral scholarship. MT was supported by a doctoral scholarship from the Alzheimer Society Canada. JV was supported by scholarships from Merck Canada, Laval University 'Fonds d'Enseignement et de Recherche', and the Fondation du CHU de Québec. All authors proofread, made comments and approved the paper.*

© 2020 The Authors. *Hepatology Communications* published by Wiley Periodicals LLC on behalf of American Association for the Study of Liver Diseases. This is an open access article under the terms of the Creative Commons Attribution–NonCommercial–NoDerivs License, which permits use and distribution in any medium, provided the original work is properly cited, the use is non-commercial and no modifications or adaptations are made.

View this article online at [wileyonlinelibrary.com](http://wileyonlinelibrary.com).

DOI 10.1002/hep4.1609

Potential conflict of interest: Dr. Marette consults and received grants from Danone Nutricia Inc., Acasti, and Allysta.

## ARTICLE INFORMATION:

From the <sup>1</sup>Centre De Recherche De L'institut De Cardiologie Et Pneumologie De Québec, Québec, Canada; <sup>2</sup>Faculté De Médecine, Université Laval, Québec, Canada; <sup>3</sup>Axe Neurosciences, Centre De Recherche du CHU de Québec-Université Laval, Québec, Canada; <sup>4</sup>Faculté De Pharmacie, Université Laval, Québec, Canada; <sup>5</sup>OptiNutriBrain International Associated Laboratory, Québec, Canada; <sup>6</sup>Laboratoire de Pharmacologie Moléculaire, Axe Endocrinologie et Néphrologie, Centre de Recherche du CHU de Québec (Pavillon CHUL), Québec, Canada; <sup>7</sup>Central Virginia VA Health Care System, Richmond, VA; <sup>8</sup>Virginia Commonwealth University, Richmond, VA.

## ADDRESS CORRESPONDENCE AND REPRINT REQUESTS TO:

Frédéric Calon, Ph.D.  
Centre De Recherche du CHU de Québec, Université Laval  
2705 Boul. Laurier  
Neurosciences, T-2-67

Québec, QC G1V 4G2, Canada  
E-mail: [Frederic.Calon@crchul.ulaval.ca](mailto:Frederic.Calon@crchul.ulaval.ca)  
Tel.: +1-418-525-4444 ext. 48697

and represent the pathway of cerebrosterol elimination through bile and urine.<sup>(17)</sup> Because the liver is the major organ involved in cerebrosterol clearance,<sup>(15)</sup> understanding how hepatic metabolism affects this metabolite might help establish it as a relevant AD biomarker.

The triple transgenic AD mouse model (3xTg-AD) reproduces both A $\beta$  and tau neuropathologies, the two main neuropathological hallmarks of AD, but also peripheral metabolic impairment such as glucose intolerance.<sup>(11,18)</sup> Because the liver plays a major role both in the regulation of glucose and lipid homeostasis, as well as in A $\beta$  and cerebrosterol metabolism, our goal was to explore the role of this key organ in the peripheral metabolic alterations found in 3xTg-AD mice and to better define the relationship between AD and NAFLD.

## Materials and Methods

### ANIMAL MODEL

The Laval University animal ethics committee approved all animal experiments. We used the triple transgenic Alzheimer's disease mouse model (3xTg-AD), which expresses three mutant genes, coding for the mutant human A $\beta$  precursor protein (APP<sup>swe</sup>), tau (P301L), and presenilin-1 (PS1 M146V).<sup>(19)</sup> The 3xTg-AD mice were produced at our animal facility, along with nontransgenic (NTg) controls with the same genetic background (C57BL6/129SvJ).<sup>(11,18)</sup> Mice received either a control diet (CD; 12% kcal fat) or a HFD (60% kcal fat) for a 9-month period starting at the age of 6 months (Research Diets, New Brunswick, NJ<sup>(11,18)</sup>). Animals were sacrificed at 15 months of age by intracardiac perfusion under deep anesthesia with ketamine/xylazine (100 mg/kg per 10 mg/kg). All groups consisted of 7–12 animals as mentioned in each figure legend, with a proportion of 70%–80% female mice (n = 5–9).

### LIVER MARKERS AND HISTOPATHOLOGY

Aspartate aminotransferase (AST) and alanine aminotransferase (ALT) were analyzed in plasma from intracardiac blood (centrifuged 5 minutes, 3,000 rpm) sampled just before intracardiac perfusion at sacrifice with a modular analyzer (Roche, Basel, Switzerland). Histopathological analyses were performed on

hematoxylin and eosin liver sections to determine the degree of hepatic steatosis (0, no; 1, mild; 2, moderate; and 3, severe hepatic steatosis) and inflammatory (0, no; 1, mild; 3, moderate; and 4, severe hepatic inflammation) grade. A liver-specialized pathologist (Dr. Lippman) blindly performed the analysis.

### LIVER TRIGLYCERIDE AND CHOLESTEROL CONTENT

Liver triglyceride (TG) and cholesterol contents were assessed following a modified Folch extraction as described previously<sup>(20)</sup> and enzymatic reactions with commercial kits (Randox Laboratories, Crumlin, United Kingdom).

### RNA EXTRACTION AND REAL-TIME POLYMERASE CHAIN REACTION

RNA was extracted using TRIzol, as per the manufacturer's instructions (Thermo Fisher Scientific, Burlington, Canada). RNA concentration and purity were assessed by measuring absorbance at 260 nm and 280 nm. A total of 2  $\mu$ g of RNA were reverse-transcribed to complementary DNA (cDNA) using a cDNA reverse-transcription kit (Applied Biosystems, Foster City, CA). The cDNA were diluted in DNase free water (1:25). Quantitative polymerase chain reaction (PCR) was performed either with TaqMan probes and primers (Applied Biosystems) or using a SYBR Green Jump-Start Gene Expression Kit (Sigma-Aldrich, Oakville, Canada). Primers are detailed in Table 1. Samples were measured in duplicate using a CFX96 or CFX384 touch real-time PCR (Bio-Rad, Mississauga, Canada). The relative expression of genes of interest was determined by normalization to two reference genes (*Hprt* and *Rpl19* for the SYBR, *Hprt* and *B2m* for the TaqMan measurements) using the comparative  $\Delta\Delta$ Ct method for relative gene expression.

### CIRCULATING AND HEPATIC A $\beta$ 42

Plasmatic and hepatic human-specific A $\beta$ 42 were measured using a human A $\beta$  enzyme-linked immunosorbent assay (ELISA) kit (Wako, Osaka, Japan) according to the manufacturer's instructions. This kit has a detection threshold of 0.1 pM.

TABLE 1. PRIMER SEQUENCES AND ASSAY IDS

Gene	Forward (5' -3')	Reverse (5' -3')
SYBR Green		
<i>Abca1</i>	Mm.PT.58.9651201	
<i>Cpt1</i>	TGCCTCTATGTGGTGTCCAA	CATGGCTTGTCTCAAGTGCT
<i>Hprt</i>	CCCCAAAATGGTTAAGGTTGC	AACAAAGTCTGGCCTGTATCC
<i>Ppargc1a</i>	TGGATGAAGACGGATTGC	TGGTTCTGAGTGCTAAGAC
<i>Ppara</i>	CTGAGACCCTCGGGAAC	AAACGTCAGTTCACAGGAAG
<i>Rpl19</i>	Mm.PT.58.12385796	
TaqMan		
<i>B2m</i>	Mm.PT.39a.22214835	
<i>Hmgcr</i>	Mm01282499_m1	
<i>Hprt</i>	Mm.PT.39a.22214828	
<i>G6pc</i>	Mm00839363_m1	
<i>Pck1</i>	Mm01247058_m1	
<i>Srebf1</i>	Mm00550338_m1	
<i>Srebf2</i>	Mm01306292_m1	

Abbreviations: *B2m*,  $\beta 2$  microglobulin; *Hprt*, hypoxanthine-guanine phosphoribosyltransferase; *Rpl19*, 60S ribosomal protein L19.

## WESTERN BLOT

Total proteins were lysed from frozen powdered livers in a radio immunoprecipitation assay buffer (50 mM tris(hydroxymethyl)aminomethane, pH = 7.4, 150 mM NaCl, 0.5 mM ethylene diamine tetraacetic acid, 5 mM ethylene glycol tetraacetic acid, 2 mM sodium orthovanadate, 50 mM sodium fluoride, 80 mM sodium  $\beta$ -glycerophosphate, 5 mM sodium pyrophosphate, 1 mM phenylmethylsulfonyl fluoride, 1% Triton-X-100, 0.1% sodium dodecyl sulphate, 1% sodium deoxycholate, and 1% protease inhibitor cocktail<sup>(21)</sup>). An equal amount of protein of 6-10 animals/group was separated by sodium dodecyl sulfate-polyacrylamide gel electrophoresis and then electroblotted onto a nitrocellulose membrane. Membranes were blocked in 5% milk powder in tris(hydroxymethyl)aminomethane-buffered saline Tween 20 for 1 hour and immunoblotted with primary antibodies overnight at 4°C, followed by horseradish peroxidase-coupled secondary antibodies for 1 hour at room temperature. Membranes were exposed to chemiluminescence reagents (EMD Millipore, Burlington, MA) and bands visualized using a BioRad imaging system and quantified with the corresponding software (ImageLab, Bio-Rad). The list of primary antibodies that were used in our experiments is available in Table 2.

TABLE 2. ANTIBODIES

Antibody	Source
pACC	Phospho-acetyl-CoA carboxylase (Ser79) #3661, Cell Signaling*
ACC	Acetyl-CoA carboxylase antibody #3662, Cell Signaling*
ACE2	Anti-ACE2 antibody (ab15348), Abcam <sup>†</sup>
eEF2	EEF2 antibody #2332, Cell Signaling*
FAS	FAS antibody #3189, Cell Signaling*
IDE	Anti-IDE antibody (ab133561), Abcam <sup>†</sup>
LRP1	Anti-LRP1 antibody [EPR3724] (ab92544), Abcam <sup>†</sup>
MitoProfile Total OXPHOS	MitoProfile total OXPHOS rodent WB antibody cocktail #MS604, MitoSciences <sup>‡</sup>
NEP	Anti-CD10 antibody [EPR2997] (ab79423), Abcam <sup>†</sup>
UGT1A	Verreault et al. <sup>(22)</sup>

\*Cell Signaling Technology, Danvers, MA.

<sup>†</sup>Abcam, Cambridge, United Kingdom.

<sup>‡</sup>MitoSciences, Eugene, OR.

Abbreviation: OXPHOS, oxidative phosphorylation.

## GLUCURONIDATION ASSAYS

Glucuronidation assays within mouse livers were performed as described by Dr. Barbier's group.<sup>(23)</sup> Briefly, enzymatic assays were performed with 24S-OH-C (2.5  $\mu$ M) at 37°C for 1 hour in the presence of 50  $\mu$ g liver homogenates in a final volume of 100  $\mu$ L of the previously reported assay buffer. Assays were ended by adding 100  $\mu$ L of methanol containing 0.02% butylated hydroxytoluene. The formation of 24S-OH-C-24G was ascertained through liquid chromatography-tandem mass spectrometry (LC/MS-MS).

## QUANTIFICATION OF 24S-OH-C AND ITS GLUCURONIDE DERIVATIVE BY LC/MS-MS

24S-OH-C, 24S-OH-C-3S, 24S-OH-C-24G, and 24S-OH-C-3S,24G were synthesized by the organic synthesis service at the CHU de Québec Research Center (<http://pfchem.crchul.ulaval.ca/en/index.html>) (Québec, Canada). [<sup>2</sup>H<sub>7</sub>]-24S-hydroxycholesterol was purchased from C/D/N Isotopes (Montréal, Canada). [<sup>2</sup>H<sub>7</sub>]-24S-hydroxycholesterol-3S, [<sup>2</sup>H<sub>7</sub>]-24S-hydroxycholesterol-24G, and [<sup>2</sup>H<sub>7</sub>]-24S-hydroxycholesterol-3S, 24G were prepared through *in vitro* enzymatic assays using liver homogenates or microsomes as reported.<sup>(23)</sup> Levels of 24S-OH-C, 24S-OH-C-24G, and 24S-OH-C-3S,24G in plasma or *in vitro*

enzymatic assays were quantified through LC/MS-MS. For 24S-OH-C quantification, the chromatographic system consisted of a Prominence UltraFast Liquid Chromatograph (Shimadzu Scientific instruments Inc., Columbia, MD), and the chromatographic separation was achieved with a Synergie RP Hydro 2.5- $\mu$ m packing material, 50  $\times$  3.0 mm (Phenomenex, Torrance, CA). Analytes were detected using an API4000 mass spectrometer (AB Sciex, Concord, Canada), operated in multiple reactions monitoring mode (MRM), and equipped with a turbo ion-spray source. Electrospray ionization was performed in positive ion mode, with voltage held at 5,500 V. 24S-OH-C-24G and 24S-OH-C-3S,24G were detected with an API3200 mass spectrometer (AB Sciex), operated in MRM mode and equipped with a turbo ion-spray source. For those compounds, the chromatographic system consisted of an Agilent 1200 apparatus (Agilent Technologies, Ville Saint-Laurent, Canada). The chromatographic separation was achieved using a Gemini C<sub>18</sub> 3- $\mu$ m packing material, 100  $\times$  4.6 mm (Phenomenex).

## STATISTICAL ANALYSES

Data are expressed as mean  $\pm$  SEM. Statistical analyses were performed using Prism 7.0a (GraphPad Software Inc., San Diego, CA). The threshold for statistical significance was set to  $P < 0.05$ . Homogeneity of variance and normality were determined for all data sets using Shapiro-Wilk's normality test. When normality of the residuals was confirmed, two-group data sets were analyzed using Student  $t$  test, and four-group data sets by a two-way analysis of variance (ANOVA) to determine the effect of the diet and genotype as well as their interaction. A one-way ANOVA with

Tukey's *post hoc* test was performed between HFD groups when main treatment or interaction effects were significant. When normality was not confirmed, data were analyzed using the Mann-Whitney U test for two-group comparisons and the Kruskal-Wallis test followed by Dunn's multiple comparison for four-group data sets, as specified in the respective figure legends. Pearson correlation coefficients were determined using simple linear regression.

## Results

### LIVER LIPIDS STORAGE IS REDUCED IN OBESE 3xTg-AD MICE

3xTg-AD mice were shown in our previous studies to be glucose-intolerant, a phenotype exacerbated following a HFD and progressing with age along with AD neuropathology.<sup>(11,18,24)</sup> Body, liver, and epididymal adipose tissue (eWAT) weights were increased by HFD in both NTg and a 3xTg-AD mice, whereas no effect of genotype was observed (Table 3). However, a tendency for decreased liver and eWAT weight was observed in obese 3xTg-AD mice compared with obese controls (Table 3). No changes were found in AST and ALT levels between groups (Fig. 1A,B), suggesting no major liver damage.

Because hepatic lipid metabolism is altered by HFD, thus contributing to impaired glucose homeostasis in this model, we next evaluated hepatic steatosis. Livers of HFD-fed NTg mice accumulated significantly more TGs than CD controls (31.7  $\pm$  4.1 mg/g tissue vs. NTg CD: 14.9  $\pm$  3.1 mg/g tissue;  $P < 0.01$ ) (Fig. 1C). This diet-induced lipid accumulation was not observed

**TABLE 3. BODY AND ORGAN WEIGHTS OF 15-MONTH-OLD NTG AND 3xTg-AD MICE FOLLOWING 9 MONTHS OF CD OR HFD**

	NTg CD	NTg HFD	3xTg-AD CD	3xTg-AD HFD	HFD Effect (PValue)	Genotype effect (PValue)	Diet-Genotype Interaction
Body weight (g)	33.46 $\pm$ 1.93	48.87 $\pm$ 2.76**	33.48 $\pm$ 1.59	44.15 $\pm$ 2.29*	<0.0001	ns	ns
Liver weight (g)	1.29 $\pm$ 0.16	1.80 $\pm$ 0.16	1.31 $\pm$ 0.10	1.57 $\pm$ 0.17	= 0.0884	ns	= 0.0700
Liver/body weight (%)	3.88 $\pm$ 0.32	3.83 $\pm$ 0.38	3.87 $\pm$ 0.16	3.41 $\pm$ 0.43	ns	ns	ns
eWAT weight (g)	1.21 $\pm$ 0.18	3.64 $\pm$ 0.43**	1.24 $\pm$ 0.24	2.77 $\pm$ 0.53*	<0.0001	ns	ns
eWAT/body weight (%)	3.69 $\pm$ 0.40	7.99 $\pm$ 1.41	3.13 $\pm$ 0.43	6.88 $\pm$ 1.15**	<0.0001	ns	ns

Note: Data are presented as mean  $\pm$  SEM (n = 7-12/group; one-way ANOVA with Tukey's *post hoc* test [liver/body weight]; Kruskal-Wallis test followed by Dunn's multiple comparison [body weight, liver weight, eWAT weight, EWAT/body weight]).

\* $P < 0.05$ , \*\* $P < 0.01$  versus respective CD group.

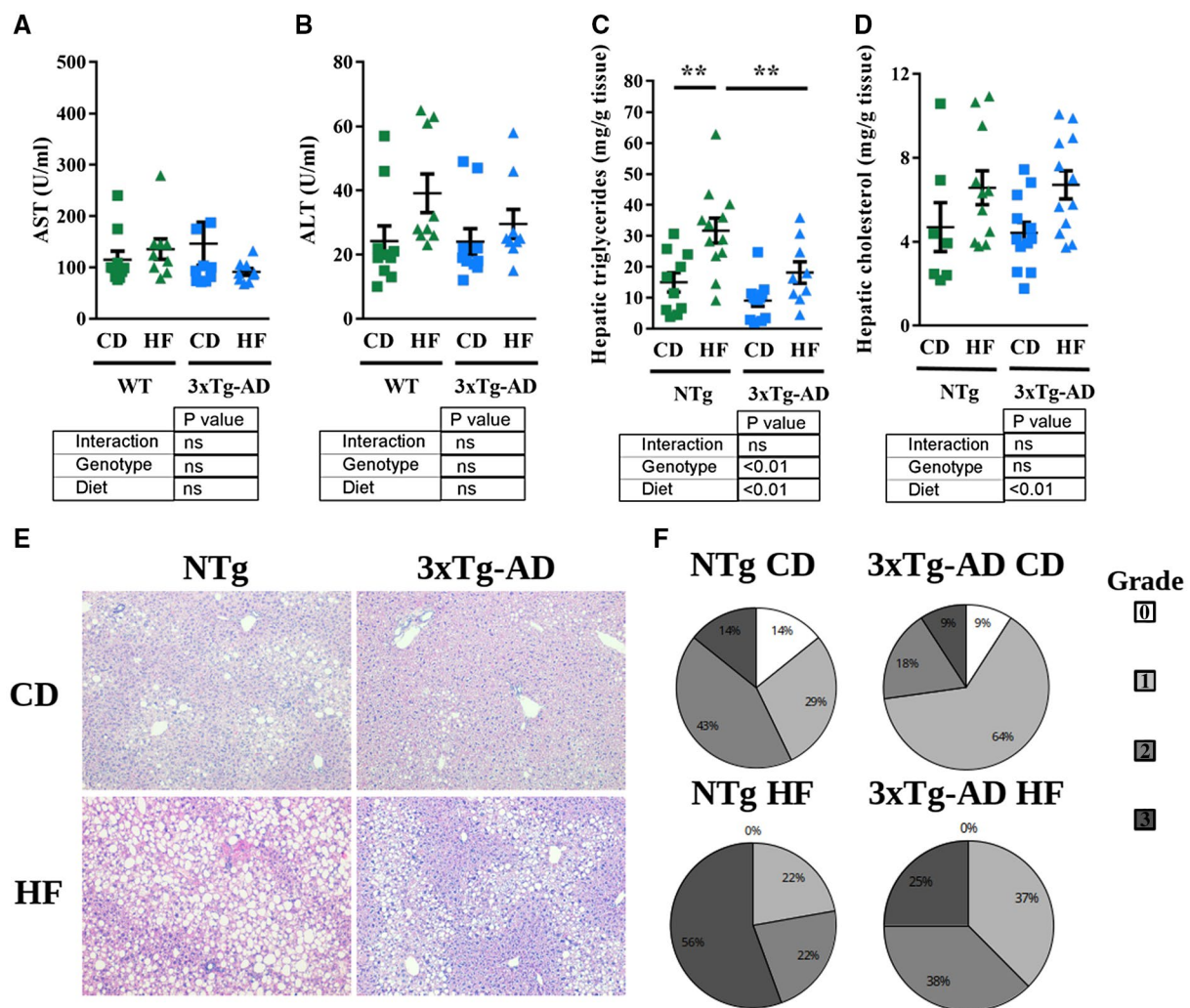


**FIG. 1.** Hepatic markers and lipid content in CD and HFD-fed NTg and 3xTg-AD mice. Circulating AST (A) and ALT (B) levels. Hepatic TG (C) and cholesterol (D) levels. (E) Representative hematoxylin and eosin-stained sections. (F) Histological steatosis score presented as percentage of mice showing the respective score for each experimental group (0, no; 1, mild; 2, moderate; and 3, severe hepatic steatosis). Data are presented as mean  $\pm$  SEM ( $n = 7$ -11/group; one-way ANOVA with Tukey's *post hoc* test;  $**P < 0.01$ ).

in obese 3xTg-AD mice ( $18.1 \pm 3.5$  mg/g tissue vs. 3xTg-AD CD:  $11.2 \pm 1.5$  mg/g tissue;  $P > 0.05$ ) (Fig. 1C). Hepatic cholesterol levels increased following HFD in both NTg and 3xTg-AD mice (Fig. 1D).

To strengthen the liver-brain relationship, we investigated the linear relationship between the previously described liver markers and cerebral concentrations of A $\beta$  in the same animals, previously published by our group.<sup>(11)</sup> Significant linear correlations were found between cortical soluble A $\beta$ 40 and A $\beta$ 42 and hepatic cholesterol, as well as between cerebral insoluble A $\beta$ 40 and A $\beta$ 42 and hepatic TGs (Table 4). AST and ALT levels did not correlate with cerebral A $\beta$ .

Histopathological analysis confirmed less severe lipid accretion in HFD-fed 3xTg-AD mice, as revealed by the lower abundance of lipid droplets and reduced steatosis scores as compared with HFD-fed NTg (25% 3xTg-AD HFD vs. 55% NTg HFD presented grade 3 steatosis) (Fig. 1E,F). Histopathological signs of inflammation were absent or minimal in all groups.

## HEPATIC METABOLISM IN OBESE 3xTg-AD MICE

To explore potential underlying mechanisms for reduced lipid storage in the liver of obese 3xTg-AD

**TABLE 4. CORRELATION BETWEEN LIVER MARKERS AND CEREBRAL A $\beta$  IN 3xTg-AD MICE FOLLOWING 9 MONTHS OF CD OR HFD**

	Soluble A $\beta$ 40 (fg/ $\mu$ g protein)	Soluble A $\beta$ 42 (fg/ $\mu$ g protein)	Insoluble A $\beta$ 40 (fg/ $\mu$ g tissue)	Insoluble A $\beta$ 42 (fg/ $\mu$ g tissue)
AST (U/mL)	+0.16 (>0.05)	+0.13 (>0.05)	+0.31 (>0.05)	+0.18 (>0.05)
ALT (U/mL)	+0.17 (>0.05)	+0.31 (>0.05)	+0.39 (>0.05)	+0.21 (>0.05)
Hepatic TGs (mg/g tissue)	+0.29 (>0.05)	+0.25 (>0.05)	<b>+0.69 (= 0.05)*</b>	<b>+0.85 (&lt;0.01)**</b>
Hepatic cholesterol (mg/g tissue)	<b>-0.73 (&lt;0.05)*</b>	<b>-0.75 (&lt;0.05)*</b>	+0.46 (>0.05)	-0.31 (>0.05)

Note: Data are presented as  $r$  correlation coefficient ( $P$  value). Values in bold are significantly correlated: \* $P < 0.05$ , \*\* $P < 0.01$ .

mice, we assessed the main hepatic pathways of lipid, glucose, and energy metabolism. Following HFD in NTg animals, protein levels of fatty acid synthase (FAS) decreased by approximately 80%; those of total acetyl-CoA carboxylase (tACC) decreased by 55%, whereas its phosphorylated form pSer79 ACC decreased by 35% (pACC) ( $P < 0.001$  vs. NTg CD) (Fig. 2A). Following HFD in 3xTg-AD mice, the same trends were observed at lower percentages (FAS: 90%, tACC: 60%, pACC: 50%, respectively;  $P < 0.001$  vs. 3xTg-AD CD); genotypic differences did not generate statistical significance ( $P > 0.05$  vs. NTg HFD) (Fig. 2A). The ratio of pACC/tACC was increased only in NTg HFD mice, accounting for increased lipogenesis. Expression of genes involved in fatty acid oxidation (*Ppara* [peroxisome proliferator-activated receptor alpha], *Ppargc1a* [peroxisome proliferative activated receptor, gamma, coactivator 1 alpha], and *Cpt1a* [carnitine palmitoyltransferase 1a]) was not significantly changed, although trends toward a genotype-diet interaction for *Ppara* ( $P = 0.0858$ ) and an HFD-induced increase for *Cpt1a* ( $P = 0.0937$ ; Fig. 2B) were seen. We next investigated the messenger RNA (mRNA) expression of gluconeogenic enzymes *Pck1* (phosphoenolpyruvate carboxykinase 1) and *G6pc* (glucose-6-phosphatase) and found that HFD decreased *Pck1* and tended to increase *G6pc* (Fig. 2C), but no genotypic effects were observed.

We next examined mitochondrial function by measuring the expression of mitochondrial OXPHOS proteins, but the expression of each of the complexes was similar between groups, although it tended to be higher in all groups compared with NTg CD (Fig. 2D).

## HEPATIC A $\beta$ METABOLISM

Because the liver is a major clearing organ for A $\beta$  peptides,<sup>(14)</sup> we investigated how HFD modulates

its clearing enzymes. Levels of plasma human A $\beta$ 42, induced only in 3xTg-AD mice, remained unaffected by the HFD (Fig. 3A). We were not able to detect human A $\beta$ 42 in the liver of 3xTg-AD mice by ELISA, nor its precursor APP by western blot or immunofluorescence (data not shown), confirming that the transgene is not expressed in peripheral organs.<sup>(11)</sup> Following HFD, we observed a reduction of insulin degrading enzyme (IDE) and a trend toward lower levels of neprilysin (NEP), the main hepatic enzymes responsible for A $\beta$  clearance, regardless of genotype (Fig. 3B,C). Angiotensin-converting enzyme 2 (ACE2), also known to play a role in degrading cerebral A $\beta$ ,<sup>(25)</sup> and the A $\beta$  receptor low-density lipoprotein receptor-related protein 1 (LRP1) were unchanged among the groups (Fig. 3B,C).

## HEPATIC 24S-OH-C METABOLISM

Circulating cholesterol was significantly increased in HFD-fed NTg mice compared with CD-fed controls, but this dietary effect was not observed in 3xTg-AD mice, which had significantly lower cholesterol levels as compared with their HFD-fed NTg counterparts (Fig. 4A). HDL cholesterol, the major cholesterol fraction in rodents, was not different among groups (NTg CD:  $1.78 \pm 0.12$  mmol/L vs. 3xTg-AD CD:  $1.31 \pm 0.06$  mmol/L, NTg HF:  $1.94 \pm 0.24$  mmol/L, 3xTg-AD HFD:  $1.31 \pm 0.21$  mmol/L,  $P > 0.05$ ). Although plasma 24S-OH-C was similar between groups, 24S-OH-C-24G plasma content was greater than 50% lower in 3xTg-AD mice without reaching statistical significance ( $P = 0.06$ ) (Fig. 4B,C). 24S-OH-C-3S,24G plasmatic levels were below the detection limit in most mice. Measurement of the production rate of these metabolites in the liver revealed that formation of 24S-OH-C-24G decreased by 30% and

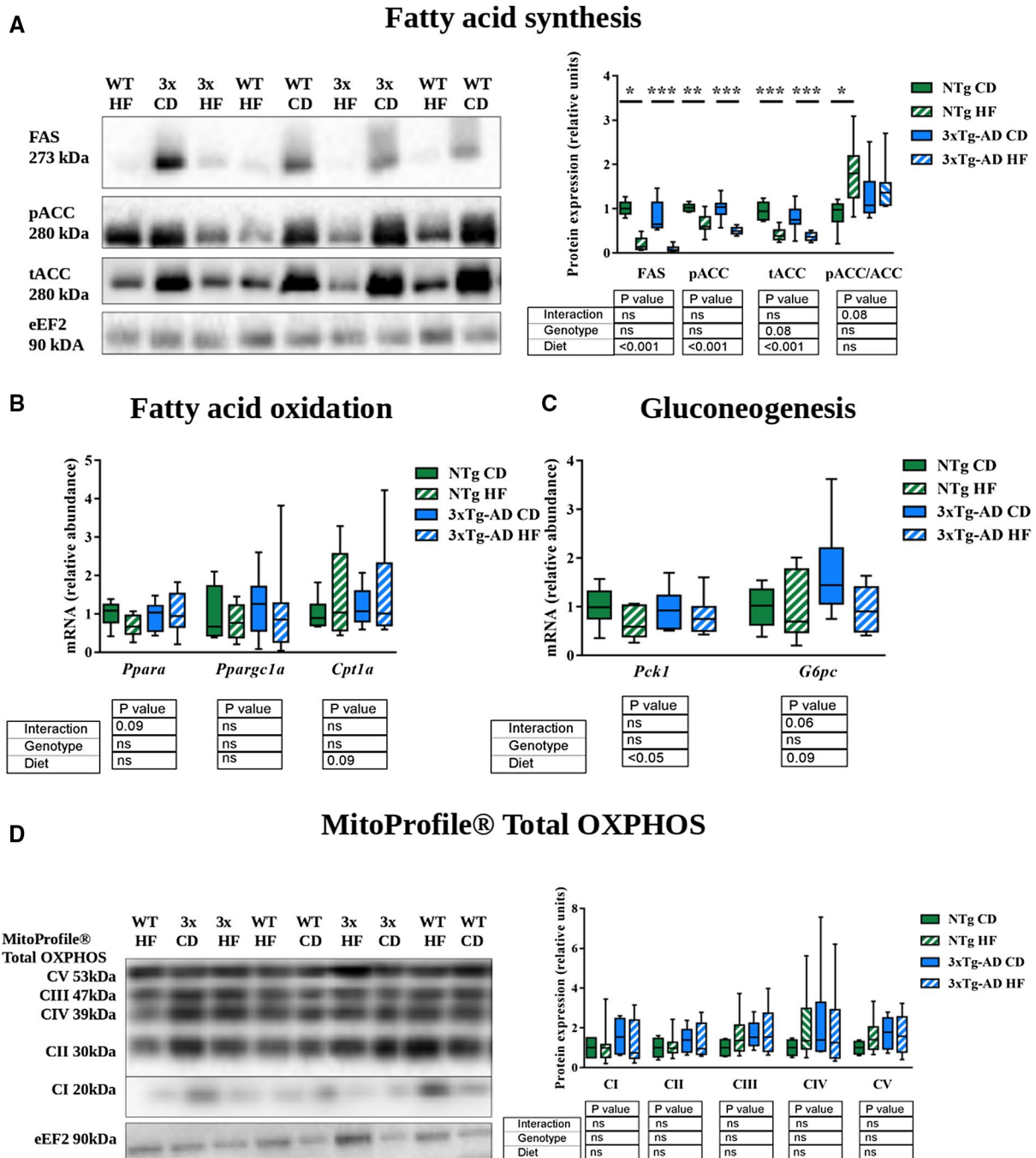


**FIG. 2.** Hepatic lipid and glucose metabolism in CD and HFD-fed NTg and 3xTg-AD mice. (A) Representative western blot images and quantification of proteins involved in lipid synthesis. (B) Expression of genes involved in fatty acid oxidation. (C) Expression of genes involved in gluconeogenesis. (D) Representative western blots and quantification of proteins of the mitochondrial respiratory complex. Data are presented as mean  $\pm$  SEM ( $n = 7-11$ /group; one-way ANOVA with Tukey's *post hoc* test [*Ppara*, *Pck1*]; Kruskal-Wallis test followed by Dunn's multiple comparison [*Ppargc1a*, *Cpt1a*]; \* $P < 0.05$ , \*\* $P < 0.01$ , \*\*\* $P < 0.001$ ). Abbreviations: CI, complex I subunit NDUF8; CII, complex II subunit 30kDa; CIII, complex III subunit core 2; CIV, complex IV subunit I; CV, ATP synthase subunit alpha; eEF2, eukaryotic elongation factor 2; and ns, not significant.

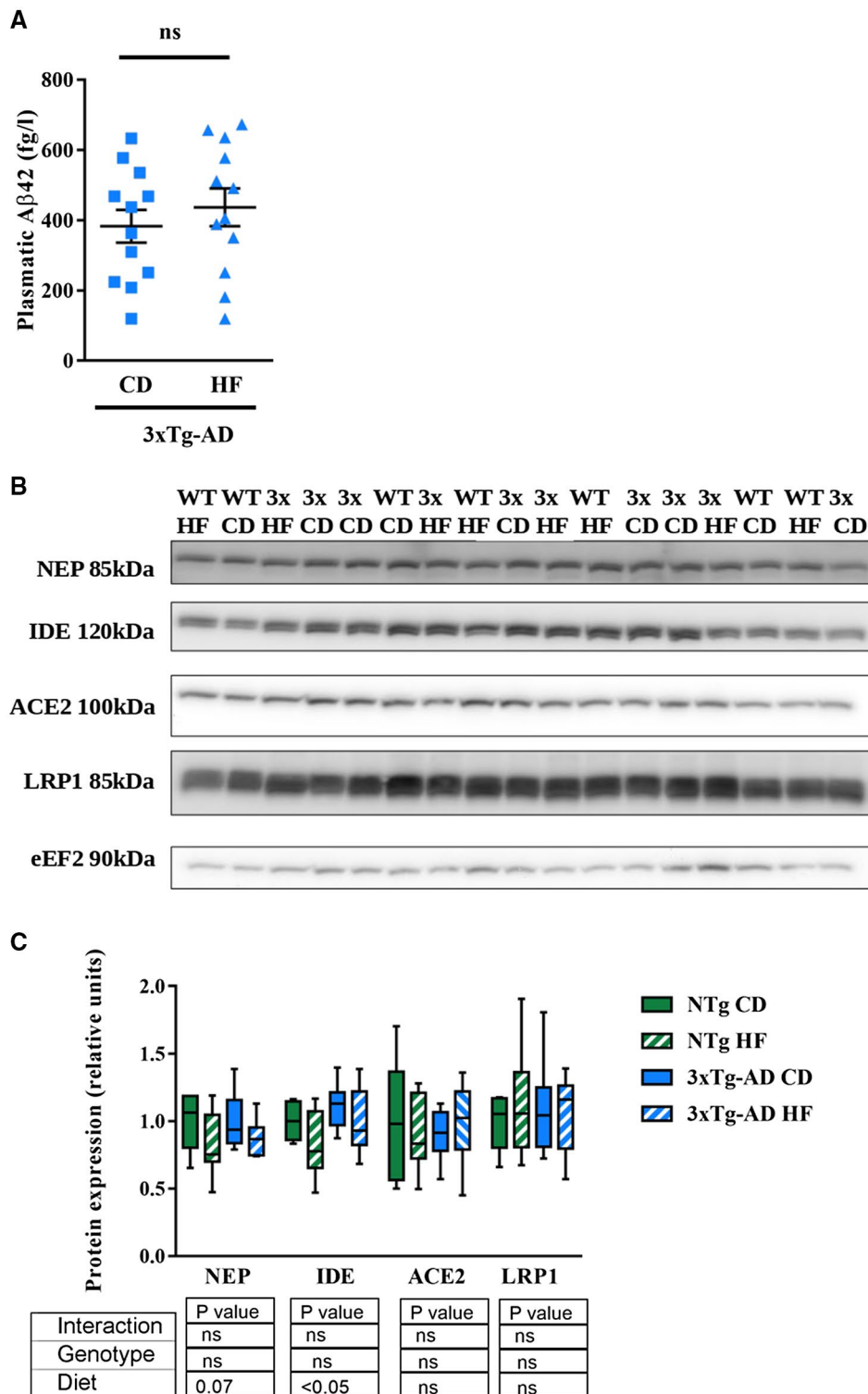


**FIG. 3.** Hepatic Aβ metabolism in 3xTg-AD mice. (A) Circulating Aβ42 levels. (B) Representative western blot images and quantification of proteins involved in Aβ clearance. (C) Quantification of proteins involved in Aβ clearance. Data are presented as mean ± SEM (n = 7-11/group; Student *t* test [plasmatic Aβ42]; one-way ANOVA with Tukey's *post hoc* test).

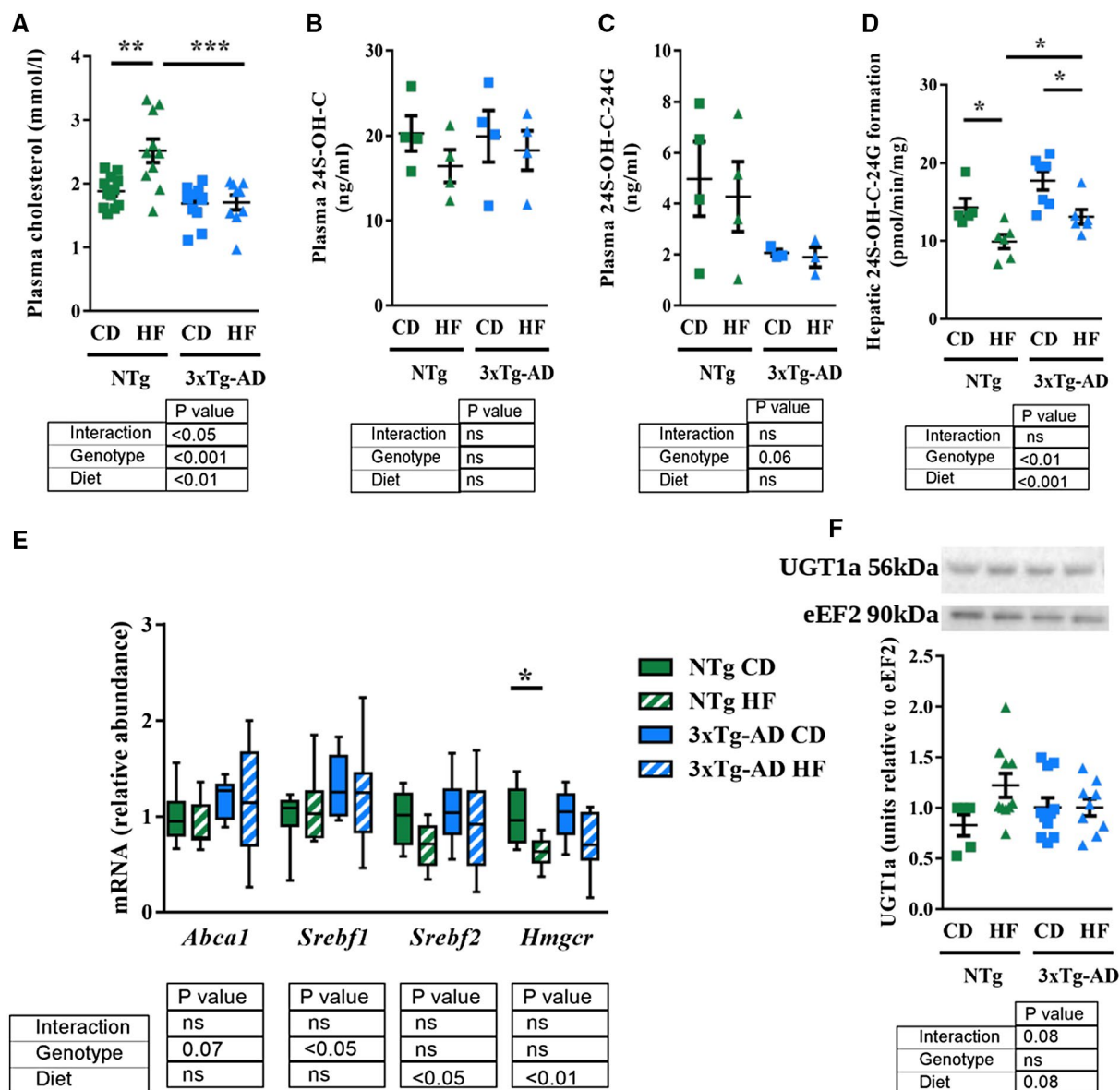


**FIG. 4.** Hepatic 24S-OH-C metabolism in NTg and 3xTg-AD mice fed a CD or HFD. Circulating cholesterol (A), 24S-OH-C (B), and 24S-OH-C-24G (C) levels. (D) Hepatic glucuronidation rate of 24S-OH-C into 24S-OH-C-24G. (E) Hepatic expression of target genes of 24S-OH-C. (F) Representative western blot and quantification of hepatic UGT1A. Data are presented as mean  $\pm$  SEM ( $n = 7-11$ /group; ANOVA with Tukey's *post hoc* test [circulating cholesterol, 24S-OH-C, circulating and hepatic 24S-OH-C-24G, *Abca1*, *Srebf2*, UGT1A]; Kruskal-Wallis test followed by Dunn's multiple comparison [*Srebf1*, *Hmgcr*]; \* $P < 0.05$ , \*\* $P < 0.01$ , \*\*\* $P < 0.001$ ).

26%, respectively, in HFD-fed NTg and 3xTg-AD mice versus their respective CD-fed controls (Fig. 4D). However, the production rate remained significantly higher in obese 3xTg-AD than in obese NTg animals ( $13.09 \pm 0.93$  pmol/min/mg in 3xTg-AD HFD vs.  $9.93 \pm 0.89$  pmol/min/mg in NTg HFD;  $P < 0.05$ ) (Fig. 4D). The rate of 24S-OH-C-3S,24G production showed similar trends, although at a

much lower level compared with 24S-OH-C-24G, and was not detectable in all mice (data not shown).

The mRNA expression of several genes known to be induced by 24S-OH-C revealed a differential modulation in the liver: *Abca1* (ATP-binding cassette transporter [member 1 of human transporter subfamily]) and *Srebf1* (sterol regulatory element-binding transcription factor 1) were both up-regulated by genotype

and not by diet, whereas *Hmgcr* (3-hydroxy-3-methylglutaryl-CoA reductase) and *Srebf2* were regulated by diet and not by genotype (Fig. 4E). Protein expression of UGT1A (UDP glucuronosyltransferase family 1 member A) was not changed (Fig. 4F).

## Discussion

This study investigated the liver implication in the peripheral metabolic dysfunction related to AD neuropathology, using the 3xTg-AD mouse model. We describe that hepatic lipid accumulation is prevented in obese 3xTg-AD mice, although fatty acid oxidation and lipogenesis were only modestly modulated. HFD-induced obesity has no impact on circulating A $\beta$ 42 levels in 3xTg-AD mice, but decreases the expression of the enzymes involved in its hepatic clearance. Obesity also lowers the hepatic glucuronidation of cerebrosterol without impacting its plasma levels. Our results advance the understanding of the relationship between peripheral metabolism and AD, which is increasingly considered a peripheral metabolic disease.<sup>(10,13,26)</sup>

### LIVER–BRAIN AXIS IN 3xTg-AD MICE

Alterations of the liver–brain axis have been described in liver diseases such as viral hepatitis and liver failure, which lead to a large spectrum of neurological abnormalities.<sup>(27,28)</sup> Cognitive impairment in these diseases worsens with age, but significantly improves after liver transplantation,<sup>(29)</sup> strengthening the role of the liver in neurological alterations. Numerous reports have emerged describing patients with NAFLD or animal models with cerebral dysfunction and neuropathology similar to AD.<sup>(6,10)</sup> A long-term HFD in normal mice induced AD-like neuropathological features in the brain; moreover, 2 months of the same diet was sufficient to accelerate plaque formation in an AD mouse model.<sup>(30)</sup> We found that liver cholesterol and TGs rather than liver markers AST and ALT correlate with cerebral A $\beta$  levels, which indicates that hepatic-induced lipid alterations, not hepatic function *per se*, is associated with brain accumulation of A $\beta$ .

Although the relationship of AD with insulin resistance and diabetes is well known,<sup>(10)</sup> the implication

of the liver–brain axis in the AD pathogenesis remains unknown. Altered liver function in patients with AD, indicated by lower albumin, increased prothrombin time and higher AST/ALT compared with control patients, has been reported.<sup>(9)</sup> Additionally, the liver function markers AST and ALT were shown to be associated with poor cognitive performance as well as with increased A $\beta$  and p-tau181 in the cerebrospinal fluid and poor cerebral glucose metabolism in patients with AD.<sup>(8)</sup> We noted no change in AST or ALT in 3xTg-AD mice, exposed or not to a HFD, consistent with previous work,<sup>(7)</sup> suggesting that AD neuropathology does not directly induce major hepatocyte damage.

### HEPATIC LIPID ACCUMULATION IS PREVENTED IN OBESE 3xTg-AD

Because lipid metabolism is implicated in the pathogenesis of AD, we investigated the effect of obesity on hepatic lipid metabolism in 3xTg-AD mice. Challenging animal models with a HFD leads to development of a NAFLD-like phenotype, with increased hepatic lipid accumulation, increased *de novo* lipogenesis, and gluconeogenesis affecting energy metabolism. Interestingly, obese 3xTg-AD mice were protected from the HFD-induced hepatic accumulation of TGs and cholesterol following modest trends in increased fatty acid oxidation and decreased lipogenesis. These results are consistent with previous studies in the amyloidopathy mouse model *APP<sub>SWE</sub>/PSEN1dE9*, in which HFD-induced hepatic lipid deposition was diminished by *de novo* lipogenesis inhibition, thus driving substrate flux toward glucose production and hyperglycemia, as well as hepatic insulin resistance and type 2 diabetes development.<sup>(12)</sup> Our previous study showed that circulating TGs are increased in obese 3xTg-AD mice.<sup>(11)</sup> Interestingly, in normal mice, TGs have been shown to cross the blood–brain barrier and induce central leptin and insulin receptor resistance, while decreasing satiety and possibly impairing cognition.<sup>(31)</sup> How this may be affected by peripheral TG alterations or neurodegenerative disease remains to be established. However, the combination of decreased liver and increased circulating TGs that we see in our obese AD mice may suggest a lipid rerouting to other organs such as the brain, but could also represent an underlying mechanism of the metabolic alterations present in these animals.

The current results indicate that hepatic fatty acid oxidation, *de novo* lipogenesis, and gluconeogenesis were affected by a high intake of saturated fat, but with no significant effect on AD transgenes. Consistent with this result, our previous study showed a similar modulation, only by diet, not by genotype, for hepatic phosphorylation of Akt 5 minutes following an intravenous insulin injection administered before sacrifice.<sup>(11)</sup>

HFD in young mice induces an increase in ACC and FAS, enzymes involved in the synthesis of fatty acids,<sup>(20)</sup> and decreased gluconeogenic enzymes *Pck1* and *G6pc*.<sup>(21)</sup> Here, we observed a marked decrease in lipogenic enzymes in both HFD groups, and a tendency toward increased *G6pc* and increased lipid oxidation in 3xTg-AD mice. Interestingly, several reports suggest that HFD started in older mice has protective effects against obesity compared with HFD started in young mice.<sup>(32,33)</sup> Moreover, the presence of physiological and physiopathological factors related to aging, such as weight loss and increased energy consumption due to development of comorbidities, could also play a role in the modulation of these hepatic metabolic enzymes.<sup>(33)</sup>

Metabolomic studies associated changes in circulating lipid compounds with cognitive status in AD, with encouraging but not fully conclusive results.<sup>(34,35)</sup> These studies did not take into consideration the peripheral metabolic status of the subjects. Because the liver plays a key role in shaping the circulating metabolome, it is logical to expect that HFD-induced hepatic changes will be reflected in blood biomarkers.

## HEPATIC A $\beta$ CLEARANCE IS DECREASED IN OBESE 3xTg-AD MICE

The 3xTg-AD mouse model was obtained by co-injecting the human mutant APP and tau transgene constructs in homozygous PS1M146V knock-in mice.<sup>(19)</sup> These mice therefore develop genetically induced A $\beta$  and tau pathologies in the brain, with no expression of the APP/Tau transgenes in the liver, whereas PS1 is ubiquitously expressed.<sup>(19)</sup> PS1 mice from the same colony do not show alteration in glucose tolerance,<sup>(24)</sup> whereas APP/PS1 mice, not expressing the tau transgene, present impaired glucose tolerance.<sup>(24)</sup> Thus, metabolic effects associated

with genotype here are likely only due to central AD pathology. In addition, among the effects of the three transgenes, sustained human A $\beta$  production was shown to play a causal role in the peripheral metabolic impairments of 3xTg-AD mice.<sup>(24)</sup>

The strong relation between type 2 diabetes and A $\beta$  is well described in the literature<sup>(2,3)</sup> and is reflected in studies in animal models. Normal mice fed a long-term HFD accumulate cerebral A $\beta$ ,<sup>(30,36)</sup> while streptozotocin-induced diabetic mice also accumulate cerebral A $\beta$  and develop memory dysfunction.<sup>(37)</sup> Inversely, transgenic mouse models overexpressing mutant A $\beta$  are glucose-intolerant even when fed a normal diet.<sup>(12)</sup> Similarly, our group established previously that 3xTg-AD mice develop glucose intolerance, which is enhanced by HFD<sup>(11)</sup> and worsens with age along with amyloid pathology.<sup>(24)</sup> This effect is partially due to an accumulation of toxic A $\beta$  of cerebral origin in the pancreas, which alters insulin secretion.<sup>(11)</sup> However, pancreatic A $\beta$  is not further enhanced in 3xTg-AD mice following a HFD, and it is believed that it only potentiates the effect of HFD on  $\beta$ -cell death.<sup>(11)</sup>

The peripheral “sink” hypothesis states that increasing the peripheral clearance of A $\beta$  could ultimately reduce its cerebral load.<sup>(38)</sup> Unfortunately, such strategies have failed in spite of efficient reduction of circulating A $\beta$ : peripherally administered NEP<sup>(39,40)</sup> or inhibition of peripheral  $\beta$ -secretase, an enzyme involved in A $\beta$  production.<sup>(38)</sup> Nevertheless, increased accumulation of A $\beta$  occurs in the brain and is aggravated by HFD,<sup>(11,18)</sup> suggesting that peripheral metabolic alterations might affect A $\beta$  degradation.

The liver is considered a major site of A $\beta$  clearance,<sup>(14)</sup> and *in vitro* studies have shown that human AD-derived liver homogenates degrade A $\beta$  at lower rates than control-derived homogenates.<sup>(14)</sup> We found that A $\beta$  generated in the brain does not accumulate a detectable amount in the liver following a HFD. Cerebral LRP1 is implicated in A $\beta$  clearance toward the periphery; in the liver, LRP1 is thought to assist other A $\beta$  clearing enzymes, such as NEP, in degrading A $\beta$ .<sup>(41)</sup> We did not find any changes in liver LRP1 among the groups. However, the two major hepatic A $\beta$  clearing enzymes, NEP and IDE, rather trended toward decreases in the liver of obese mice. This diet-specific effect suggests that impaired hepatic clearance of A $\beta$  in obese 3xTg-AD mice—in spite of similar circulating levels as lean 3xTg-AD

mice—may contribute to its cerebral and pancreatic accumulation. The recent study mentioned showed decreased IDE levels and no significant change in NEP in liver samples of patients with AD compared to controls with no AD, in accordance with our data.<sup>(14)</sup> However, patients in this study were not stratified by the presence of peripheral metabolic alterations.

Overall, our current results in animals combined with previous studies in livers of patients with AD suggest that the contribution of obesity and diabetes on hepatic A $\beta$ -degrading enzymes and AD pathology deserve to be further investigated.

### HEPATIC CEREBROSTEROL GLUCURONIDATION IS DECREASED IN OBESE 3xTg-AD MICE

Lipid species such as cholesterol, oxysterols, fatty acids, sphingolipids, and phospholipids have been investigated as biomarkers or therapeutic targets.<sup>(34,42,43)</sup> The fact that the liver is a central organ in lipid metabolism raised the hypothesis that it may play a role in modulating circulating lipids in AD and that liver dysfunction potentially affects lipid biomarkers. Previous reports showing that obesity-increased hepatic ceramides contribute to the pathogenesis of AD neurodegeneration<sup>(43)</sup> sustain this hypothesis.

Plasma cholesterol reflects hepatic synthesis, whereas cerebrosterol reflects both brain and liver cholesterol metabolism. In lean and obese 3xTg-AD mice, plasma cholesterol did not differ from NTg controls, although hepatic levels and *Hmgcr* expression were increased by diet in obese versus lean mice.

Cerebral cerebrosterol in normal mice fed a HFD for 16 weeks did not change, while circulating levels significantly decreased by 50%.<sup>(44)</sup> These changes were not accompanied by modifications of bile acids; thus, hepatic glucuronidation might account for this difference. Hepatic metabolism of different oxysterols is altered following HFD<sup>(44)</sup>; however, our study specifically shows hepatic cerebrosterol glucuronidation to be decreased in obesity. Because 24S-OH-C-3S,24G is formed through sulfonation of 24S-OH-C-24G, its limited formation is believed to reflect limited sulfonation ability in mouse liver.

Cerebrosterol is known to activate the UGT1A3,<sup>(22)</sup> while UGT1A4 is the main enzyme contributing to its glucuronidation in humans; however, the presence of missense mutations in the murine *Ugt1a4* gene leads to the absence of its homolog in the mouse liver (Dr. Barbier's group, unpublished data). Neither diet nor the triple transgenic genotype had an effect on UGT1A total protein levels, so the role of the different isoforms remains to be elucidated.<sup>(45)</sup> Moreover, 24S-OH-C plays a minor role in modulating target metabolic genes in the context of obesity, in which numerous other factors are also contributing.<sup>(46,47)</sup>

Circulating cerebrosterol is believed to reflect the mass of active neurons and is reduced in neurodegenerative disease proportionally to disease burden.<sup>(15,48)</sup> In our study, HFD decreased hepatic cerebrosterol glucuronidation in 3xTg-AD mice, without affecting its circulating levels. This implies caution when interpreting how blood measurements reflect pathology; specifically, interorgan crosstalk as well as general context should be properly evaluated. Further studies are needed to determine whether the clearance of cerebrosterol into bile acids could contribute to maintaining its circulating levels.

A potential limitation of our study is the ratio between male and female mice in our groups, which favors the latter. We performed an analysis of sex-driven effects on liver TGs and cholesterol but did not observe major differences (data not shown). Statistical power, however, was very limited for such an analysis. AD features are known to be different between males and females, with females being more susceptible to brain A $\beta$  accumulation.<sup>(24,48)</sup> Metabolic features are also different: Young and fertile female mice are protected from NAFLD development, whereas later in life ovarian senescence is strongly associated with severe liver steatosis.<sup>(49)</sup> However, in humans, cumulative incidences of dementia calculated based on age, differential mortality, and presence of risk factors are similar in women and men.<sup>(50)</sup> Because we debuted the diet assignment at an advanced age and our mice were sacrificed at an old, postmenopausal age and showed no differences in hepatic lipid measures at sacrifice, we included both female and male mice in all analyses.

In conclusion, our study sheds light on the liver-brain axis and strengthens the link between central

AD pathology and liver dysfunction, providing potential routes of explanation for peripheral metabolic impairment associated with AD. We show that modulation of hepatic lipid, A $\beta$ , and cerebrosterol metabolism in obese 3xTg-AD mice differs from control mice, suggesting that long-time presence of NAFLD can modulate peripheral AD features. These results potentially explain why many biomarkers have not been consistently correlated with AD and why certain therapeutic strategies showed beneficial effects only in particular experimental conditions or patient subgroups. Although these aspects remain to be confirmed in patients with AD, peripheral metabolic context, including liver function, should be taken into consideration when investigating potential markers or therapeutic targets in AD.

## REFERENCES

- Argo CK, Caldwell SH. Epidemiology and natural history of non-alcoholic steatohepatitis. *Clin Liver Dis* 2009;13:511-531.
- Atti AR, Valente S, Iodice A, Caramella I, Ferrari B, Albert U, et al. Metabolic syndrome, mild cognitive impairment, and dementia: a meta-analysis of longitudinal studies. *Am J Geriatr Psychiatry* 2019;27:625-637.
- Serrano-Pozo A, Growdon JH. Is Alzheimer's disease risk modifiable? *J Alzheimers Dis* 2019;67:795-819.
- Celikbilek A, Celikbilek M, Bozkurt G. Cognitive assessment of patients with nonalcoholic fatty liver disease. *Eur J Gastro Hepatol* 2018;30:944-950.
- Filipović B, Marković O, Đurić V, Filipović B. Cognitive changes and brain volume reduction in patients with nonalcoholic fatty liver disease. *Can J Gastroenterol Hepatol* 2018;2018:9638797.
- Seo SW, Gottesman RF, Clark JM, Hernaez R, Chang Y, Kim C, et al. Nonalcoholic fatty liver disease is associated with cognitive function in adults. *Neurology* 2016;86:1136-1142.
- Tournissac M, Vandal M, Tremblay C, Bourassa P, Vancassel S, Emond V, et al. Dietary intake of branched-chain amino acids in a mouse model of Alzheimer's disease: effects on survival, behavior, and neuropathology. *Alzheimers Dement (N Y)* 2018;4:677-687.
- Nho K, Kueider-Paisley A, Ahmad S, MahmoudianDehkordi S, Arnold M, Risacher SL, et al. Association of altered liver enzymes with Alzheimer disease diagnosis, cognition, neuroimaging measures, and cerebrospinal fluid biomarkers. *JAMA Netw Open* 2019;2:e197978.
- Giambattistelli F, Bucossi S, Salustri C, Panetta V, Mariani S, Siotto M, et al. Effects of hemochromatosis and transferrin gene mutations on iron dyshomeostasis, liver dysfunction and on the risk of Alzheimer's disease. *Neurobiol Aging* 2012;33:1633-1641.
- de la Monte SM, Longato L, Tong M, Wands JR. Insulin resistance and neurodegeneration: roles of obesity, type 2 diabetes mellitus and non-alcoholic steatohepatitis. *Curr Opin Investig Drugs* 2009;10:1049-1060.
- Vandal M, White PJ, Tremblay C, St-Amour I, Chevrier G, Emond V, et al. Insulin reverses the high-fat diet-induced increase in brain A $\beta$  and improves memory in an animal model of Alzheimer disease. *Diabetes* 2014;63:4291-4301.
- Tang Y, Peng Y, Liu J, Shi L, Wang Y, Long J, et al. Early inflammation-associated factors blunt sterol regulatory element-binding proteins-1-mediated lipogenesis in high-fat diet-fed APPSWE/PSEN1dE9 mouse model of Alzheimer's disease. *J Neurochem* 2016;136:791-803.
- Ferreira LSS, Fernandes CS, Vieira MNN, De Felice FG. Insulin resistance in Alzheimer's disease. *Front Neurosci* 2018;12:830.
- Maarouf CL, Walker JE, Sue LI, Dugger BN, Beach TG, Serrano GE. Impaired hepatic amyloid-beta degradation in Alzheimer's disease. *PLoS One* 2018;13:e0203659.
- Leoni V, Caccia C. 24S-hydroxycholesterol in plasma: a marker of cholesterol turnover in neurodegenerative diseases. *Biochimie* 2013;95:595-612.
- Wood WG, Li L, Müller WE, Eckert GP. Cholesterol as a causative factor in Alzheimer disease: a debatable hypothesis. *J Neurochem* 2014;129:559-572.
- Björkhem I. Crossing the barrier: oxysterols as cholesterol transporters and metabolic modulators in the brain. *J Intern Med* 2006;260:493-508.
- Julien C, Tremblay C, Phivilay A, Berthiaume L, Emond V, Julien P, et al. High-fat diet aggravates amyloid-beta and tau pathologies in the 3xTg-AD mouse model. *Neurobiol Aging* 2010;31:1516-1531.
- Oddo S, Caccamo A, Shepherd JD, Murphy MP, Golde TE, Kaye R, et al. Triple-transgenic model of Alzheimer's disease with plaques and tangles: intracellular A $\beta$  and synaptic dysfunction. *Neuron* 2003;39:409-421.
- Xu E, Forest M-P, Schwab M, Avramoglu RK, St-Amant E, Caron AZ, et al. Hepatocyte-specific Ptpn6 deletion promotes hepatic lipid accretion, but reduces NAFLD in diet-induced obesity: potential role of PPAR $\gamma$ . *Hepatology* 2014;59:1803-1815.
- Shum M, Bellmann K, St-Pierre P, Marette A. Pharmacological inhibition of S6K1 increases glucose metabolism and Akt signalling in vitro and in diet-induced obese mice. *Diabetologia* 2016;59:592-603.
- Verreault M, Senekeo-Effenberger K, Trottier J, Bonzo JA, Bélanger J, Kaeding J, et al. The liver X-receptor alpha controls hepatic expression of the human bile acid-glucuronidating UGT1A3 enzyme in human cells and transgenic mice. *Hepatology* 2006;44:368-378.
- Perreault M, Wunsch E, Bialek A, Trottier J, Verreault M, Caron P, et al. Urinary elimination of bile acid glucuronides under severe cholestatic situations: contribution of hepatic and renal glucuronidation reactions. *Can J Gastroenterol Hepatol* 2018;2018:8096314.
- Vandal M, White PJ, Chevrier G, Tremblay C, St-Amour I, Planel E, et al. Age-dependent impairment of glucose tolerance in the 3xTg-AD mouse model of Alzheimer's disease. *FASEB J* 2015;29:4273-4284.
- Evans CE, Miners JS, Piva G, Willis CL, Heard DM, Kidd EJ, et al. ACE2 activation protects against cognitive decline and reduces amyloid pathology in the Tg2576 mouse model of Alzheimer's disease. *Acta Neuropathol* 2020;139:485-502.
- Wijesekara N, Gonçalves RA, De Felice FG, Fraser PE. Impaired peripheral glucose homeostasis and Alzheimer's disease. *Neuropharmacology* 2018;136:172-181.
- Mathew S, Faheem M, Ibrahim SM, Iqbal W, Rauff B, Fatima K, et al. Hepatitis C virus and neurological damage. *World J Hepatol* 2016;8:545-556.
- Bosoi CR, Rose CF. Brain edema in acute liver failure and chronic liver disease: similarities and differences. *Neurochem Int* 2013;62:446-457.
- Acharya C, Wade JB, Fagan A, White M, Gavis E, Ganapathy D, et al. Overt hepatic encephalopathy impairs learning on the

- encephalapp stroop which is reversible after liver transplant. *Liver Transpl* 2017;23:1396-1403.
- 30) Kim D-G, Krenz A, Toussaint LE, Maurer KJ, Robinson S-A, Yan A, et al. Non-alcoholic fatty liver disease induces signs of Alzheimer's disease (AD) in wild-type mice and accelerates pathological signs of AD in an AD model. *J Neuroinflammation* 2016;13:1.
  - 31) Banks WA, Farr SA, Salameh TS, Niehoff ML, Rhea EM, Morley JE, et al. Triglycerides cross the blood-brain barrier and induce central leptin and insulin receptor resistance. *Int J Obes (Lond)* 2018;42:391-397.
  - 32) De Leon ER, Brinkman JA, Fenske RJ, Gregg T, Schmidt BA, Sherman DS, et al. Age-dependent protection of insulin secretion in diet induced obese mice. *Sci Rep* 2018;8:17814.
  - 33) Vercauteren E, Vranckx C, Frederix L, Lox M, Lijnen HR, Scroyen I, et al. Advanced-age C57BL/6J mice do not develop obesity upon western-type diet exposure. *Adipocyte* 2019;8:105-113.
  - 34) Zarrouk A, Debbabi M, Bezine M, Karym EM, Badreddine A, Rouaud O, et al. Lipid biomarkers in Alzheimer's disease. *Curr Alzheimer Res* 2018;15:303-312.
  - 35) Barupal DK, Fan S, Wancewicz B, Cajka T, Sa M, Showalter MR, et al. Generation and quality control of lipidomics data for the Alzheimer's disease neuroimaging initiative cohort. *Sci Data* 2018;5:180263.
  - 36) Busquets O, Ettcheto M, Pallàs M, Beas-Zarate C, Verdaguer E, Auladell C, et al. Long-term exposition to a high fat diet favors the appearance of  $\beta$ -amyloid depositions in the brain of C57BL/6J mice. A potential model of sporadic Alzheimer's disease. *Mech Ageing Dev* 2017;162:38-45.
  - 37) Kang S, Kim C-H, Jung H, Kim E, Song H-T, Lee JE. Agmatine ameliorates type 2 diabetes induced Alzheimer's disease-like alterations in high-fat diet-fed mice via reactivation of blunted insulin signalling. *Neuropharmacology* 2017;113:467-479.
  - 38) Georgievska B, Gustavsson S, Lundkvist J, Neelissen J, Eketjäll S, Ramberg V, et al. Revisiting the peripheral sink hypothesis: inhibiting BACE1 activity in the periphery does not alter  $\beta$ -amyloid levels in the CNS. *J Neurochem* 2015;132:477-486.
  - 39) Walker JR, Pacoma R, Watson J, Ou W, Alves J, Mason DE, et al. Enhanced proteolytic clearance of plasma A $\beta$  by peripherally administered neprilysin does not result in reduced levels of brain A $\beta$  in mice. *J Neurosci* 2013;33:2457-2464.
  - 40) Henderson SJ, Andersson C, Narwal R, Janson J, Goldschmidt TJ, Appelkvist P, et al. Sustained peripheral depletion of amyloid- $\beta$  with a novel form of neprilysin does not affect central levels of amyloid- $\beta$ . *Brain* 2014;137:553-564.
  - 41) Dries DR, Yu G, Herz J. Extracting  $\beta$ -amyloid from Alzheimer's disease. *Proc Natl Acad Sci U S A* 2012;109:3199-3200.
  - 42) Wong MW, Braidy N, Poljak A, Pickford R, Thambisetty M, Sachdev PS. Dysregulation of lipids in Alzheimer's disease and their role as potential biomarkers. *Alzheimers Dement* 2017;13:810-827.
  - 43) **Lyn-Cook LE, Lawton M**, Tong M, Silbermann E, Longato L, Jiao P, et al. Hepatic ceramide may mediate brain insulin resistance and neurodegeneration in type 2 diabetes and non-alcoholic steatohepatitis. *J. Alzheimers Dis* 2009;16:715-729.
  - 44) **Guillemot-Legrès O, Mutemberezi V**, Cani PD, Muccioli GG. Obesity is associated with changes in oxysterol metabolism and levels in mice liver, hypothalamus, adipose tissue and plasma. *Sci Rep* 2016;6:19694.
  - 45) Meech R, Hu DG, McKinnon RA, Mubarakah SN, Haines AZ, Nair PC, et al. The UDP-glycosyltransferase (UGT) superfamily: new members, new functions, and novel paradigms. *Physiol Rev* 2019;99:1153-1222.
  - 46) Schmitz G, Buechler C. ABCA1: regulation, trafficking and association with heteromeric proteins. *Ann Med* 2002;34:334-347.
  - 47) Shimano H, Sato R. SREBP-regulated lipid metabolism: convergent physiology - divergent pathophysiology. *Nat Rev Endocrinol* 2017;13:710-730.
  - 48) **Bories C, Guitton MJ**, Julien C, Tremblay C, Vandal M, Msaid M, et al. Sex-dependent alterations in social behaviour and cortical synaptic activity coincide at different ages in a model of Alzheimer's disease. *PLoS One* 2012;7:e46111.
  - 49) **Ballestri S, Nascimbeni F**, Baldelli E, Marrazzo A, Romagnoli D, Lonardo A. NAFLD as a sexual dimorphic disease: role of gender and reproductive status in the development and progression of nonalcoholic fatty liver disease and inherent cardiovascular risk. *Adv Ther* 2017;34:1291-1326.
  - 50) **Chêne G, Beiser A**, Au R, Preis SR, Wolf PA, Dufouil C, et al. Gender and incidence of dementia in the Framingham Heart Study from mid-adult life. *Alzheimers Dement* 2015;11:310-320.

Author names in bold designate shared co-first authorship.